AIP | Applied Physics Letters

Free-standing optofluidic waveguides formed on patterned superhydrophobic surfaces

Alexandr Jonáš, Berna Yalizay, Selcuk Akturk, and Alper Kiraz

Citation: Applied Physics Letters **104**, 091123 (2014); doi: 10.1063/1.4867887
View online: http://dx.doi.org/10.1063/1.4867887
View Table of Contents: http://scitation.aip.org/content/aip/journal/apl/104/9?ver=pdfcov
Published by the AIP Publishing

Free-standing optofluidic waveguides formed on patterned superhydrophobic surfaces

Alexandr Jonáš,[1,2,a)] Berna Yalizay,[1] Selcuk Akturk,[1] and Alper Kiraz[2]
[1]*Department of Physics, Istanbul Technical University, 34469 Maslak, Istanbul, Turkey*
[2]*Department of Physics, Koç University, Rumelifeneri Yolu, 34450 Sariyer, Istanbul, Turkey*

(Received 6 November 2013; accepted 24 February 2014; published online 6 March 2014)

We report on the preparation and characterization of free-standing optofluidic waveguides created on solid superhydrophobic (SH) substrates with patterned wetting properties. In order to locally modify the liquid-solid contact angle, we employed selective laser ablation of SH layers deposited on magnesium-fluoride substrates with low refractive index. Upon ablation, surfaces with hydrophilic channels surrounded by SH areas were obtained. Subsequently, we created liquid optical waveguides based on total internal reflection using ethylene glycol, a polar liquid with high refractive index spreading spontaneously along the hydrophilic surface channels. We evaluated the light guiding performance and losses of these optofluidic waveguides. © *2014 AIP Publishing LLC*. [http://dx.doi.org/10.1063/1.4867887]

Fluid-based optical components benefit greatly from the unique material properties of fluids, in particular, their large flexibility in shape accompanied by exceptionally smooth interfaces and a wide range of available refractive indices. In combination with micron-scale manipulation of the fluid flow and controlled *in situ* fluid mixing, it is possible to create reconfigurable optical systems that cannot be realized with classical solid-state materials.[1,2] Moreover, the sensitivity of the fluid shape and/or refractive index to the environmental stimuli plays the key role in the applications of optofluidic elements in sensing and actuation.[3,4]

In a typical optofluidic platform, a glass, polymer, or semiconductor chip with a system of closed microchannels provides confinement for the fluid that is then actuated through the channels using external pumping.[5,6] While this approach is quite robust, manufacturing of such devices is often rather involved and the accessibility of the fluid interface is obstructed by the solid walls of the chip. Alternatively, fluid confinement and guiding can be realized by patterning the wetting properties of a solid substrate.[7,8] In this configuration, polar liquids (such as water) are confined to the hydrophilic parts of the patterned surface whereas the hydrophobic parts serve as virtual channel walls arising from the surface tension of the liquid.[9,10] Main advantages of such systems are their easy fabrication, possibility of creating complex networks of interconnected microchannels, direct access to the liquid surface, and liquid self-actuation due to the spontaneous wetting of the hydrophilic parts of the surface.[11] However, even though surface microfluidic systems have been successfully demonstrated, their use in optofluidics has not been explored to date.

In this Letter, we demonstrate fabrication of optofluidic waveguides on superhydrophobic (SH) surfaces with patterned wetting properties. High liquid-solid contact angle of basic SH surfaces is provided by a thin layer of hydrophobic silica nanoparticles coated on planar magnesium fluoride (MgF_2) substrates with a low index of refraction. Subsequently, contact angle is locally modified by selective ablation of the SH layer with a focused femtosecond (fs) laser beam. Such selective ablation process allows to write arbitrarily shaped hydrophilic patterns on the surface. Upon deposition of ethylene glycol—polar liquid with a high index of refraction—liquid filaments form on the hydrophilic parts of the surface. Contrast of refractive index between ethylene glycol and MgF_2 then leads to confinement of light in the liquid due to total internal reflection, thus permitting light guiding. We characterize light propagation and optical losses of such free-standing optofluidic waveguides and show that they compare favorably to hydrogel-based waveguides.[12]

The starting SH substrates were prepared by spin-coating a solution of hydrophobic silica nanoparticles (Aeroxide LE1, average particle size 14 ± 3 nm; Evonik) in ethanol on the surface of cleaned crystalline MgF_2 plates (diameter 20 mm, thickness 1 mm; Crystran).[13] In order to generate a surface with uniform texture and wetting properties, the nanoparticle solution was sonicated and centrifuged prior to spin-coating to remove particle clusters and other possible contaminants. For routine characterization of the wetting properties of SH surfaces, we prepared the same type of SH surfaces spin-coated on cleaned glass cover slips. Besides being disposable, SH-coated glass cover slips show contact angles that are very similar to those observed on SH-coated MgF_2 plates. Contact angle of ethylene glycol on glass-based SH surfaces was determined by direct imaging of millimeter-sized ethylene glycol droplets deposited on the surface and analysis of the recorded droplet images. The measured contact angle of $(134.9 \pm 5.5)^\circ$ (20 measurements on 2 different SH surfaces) was significantly higher than the contact angle of ethylene glycol on a clean, hydrophilic MgF_2 surface ($<20^\circ$). Subsequently, hydrophilic patterns were created on coated MgF_2 substrates by locally ablating the SH layer with a focused fs pulsed laser beam (see Fig. 1(a)). The laser system used in the experiments (s–Pulse; Amplitude Systemes) generated 550 fs pulses at the output wavelength of 1030 nm, with 1 kHz pulse repetition rate. During the ablation process, accidental damage to the substrate should be avoided. Thus, laser fluence at the

[a)]Author to whom correspondence should be addressed. Electronic mail: ajonas@itu.edu.tr

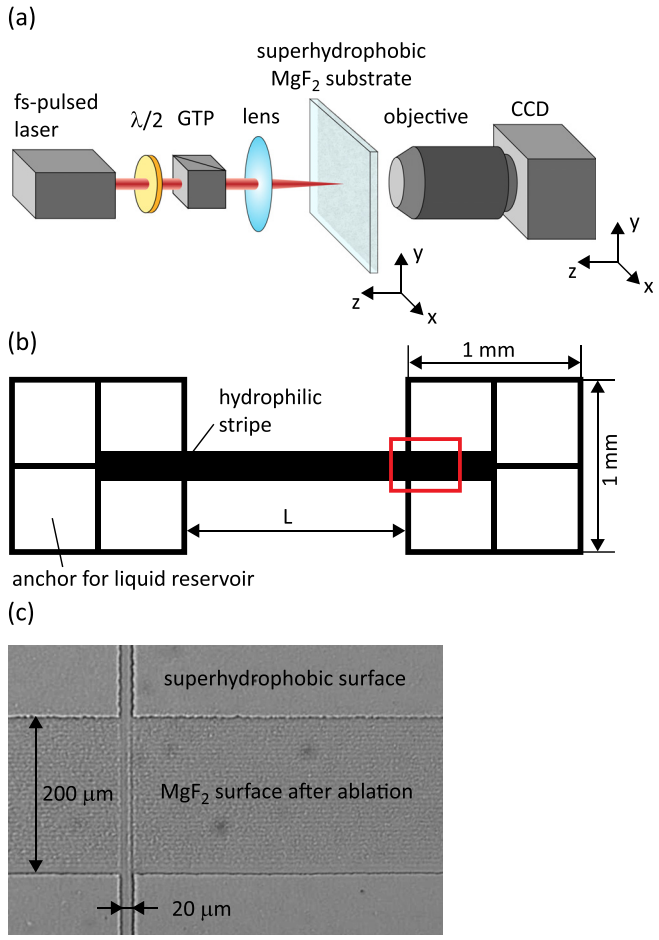

FIG. 1. (a) Experimental setup for patterning of SH surfaces with fs laser ablation. $\lambda/2$—half-wave plate, GTP—Glan-Taylor prism. (b) Schematics of patterns written on SH surfaces. *L*—length of the waveguiding region. (c) Micrograph of actual ablated SH surface within the red rectangular region indicated in (b).

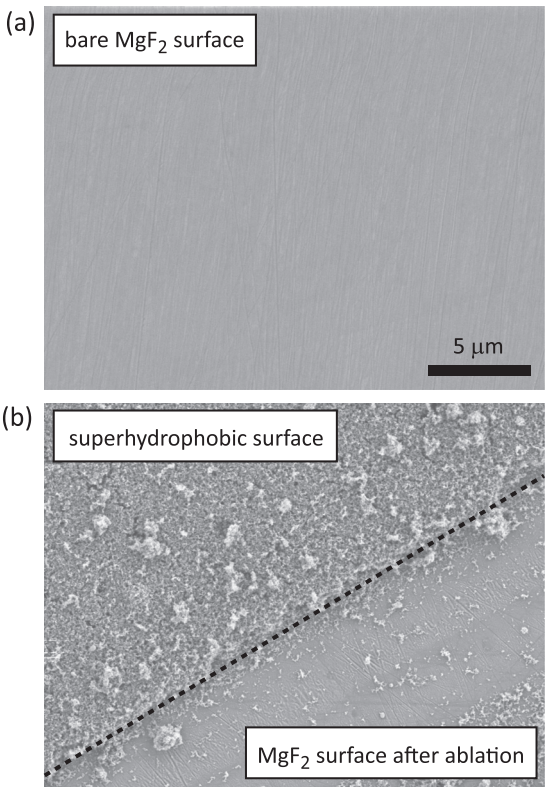

FIG. 2. (a) SEM image of bare MgF_2 surface before deposition of SH layer. (b) SEM image of superhydrophobic surface before (top left part) and after (bottom right part) the laser ablation. Dashed line denotes boundary of the ablated region.

focus should be above the ablation threshold of SH layer (silica), yet below that of MgF_2. At wavelengths around 1030 nm, the reported ablation thresholds of the two materials are very similar, yielding a tight range of adjustment. The difference between the thresholds increases significantly at shorter wavelengths.[14] To exploit this, we generated second harmonic of the laser output (515 nm) and obtained a better contrast of laser fluence with easier adjustment of the ablation operating point. The pulse energy at the second harmonic was around 30 μJ. The laser beam was focused on the surface using a double-convex spherical lens with 75 mm focal length. We observed that irradiating the SH layer through the MgF_2 plate yielded better results with almost complete removal of the silica nanoparticles and minimal modification of the refractive index and surface roughness of the MgF_2 plate (see Figs. 1(c) and 2). This was caused by beam self-focusing within the MgF_2 substrate which increased the laser fluence at the rear surface of the plate (with respect to the beam propagation direction) while also decreasing the risk of laser-induced modifications in the bulk of the substrate, as the fluence reached ablation levels only in the vicinity of the rear surface of the sample.[15] The sample with SH surface layer was mounted on a 3-axis motorized scanning stage (PT3; Thorlabs) that translated the sample past a stationary ablation beam with a constant scanning speed of 1 mm/s, thus facilitating ablation of arbitrary patterns into the surface. During the laser patterning, we simultaneously monitored the sample surface through a microscope objective with long working distance and a CCD camera. Using the method outlined above, we generated dumbbell-shaped patterns that consisted of liquid-guiding hydrophilic stripes connected to closed rectangular grids at each end (see Fig. 1(b)). These grids were used as anchors for depositing a droplet of ethylene glycol on the surface that subsequently served as a liquid reservoir for filling up the stripes with the liquid by assisted surface wetting (see below). For each pattern, a straight or curved hydrophilic stripe with a total width of ~150–200 μm and length varying between 1 and 4 mm was created between the two anchor regions.

Free-standing optofluidic waveguides were formed on patterned SH MgF_2 plates by controlled spreading of ethylene glycol along ablated hydrophilic stripes. Contrast of wettability of intact SH surface and ablated regions stems from the combined effect of hydrophobicity and submicron-scale roughness of the silica nanoparticle layer[13] (compare Figs. 2(a) and 2(b)). Figure 3(a) illustrates the geometry used for liquid deposition. A droplet of ethylene glycol was placed on the ablated anchor and a liquid filament was then created using a "dip-pen" technique: a piece of cleaned hydrophilic optical fiber was inserted into the droplet and subsequently translated along the stripe, drawing the liquid along. Figures 3(b) and 3(c) show a patterned region on SH surface indicated by a red rectangle in Fig. 3(a) before and after ethylene glycol deposition, respectively.

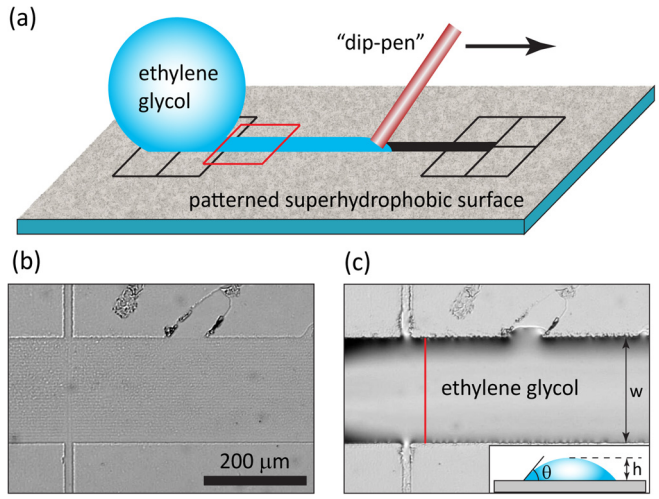

FIG. 3. (a) Selective wetting of a patterned SH surface by ethylene glycol. (b) Detail of patterned SH surface within the red rectangular region indicated in (a) before ethylene glycol deposition. (c) The same surface region as in (b) after ethylene glycol deposition. Inset illustrates cross-sectional profile of ethylene glycol filament along the red vertical line. θ denotes the apparent lateral contact angle of ethylene glycol on the patterned surface.

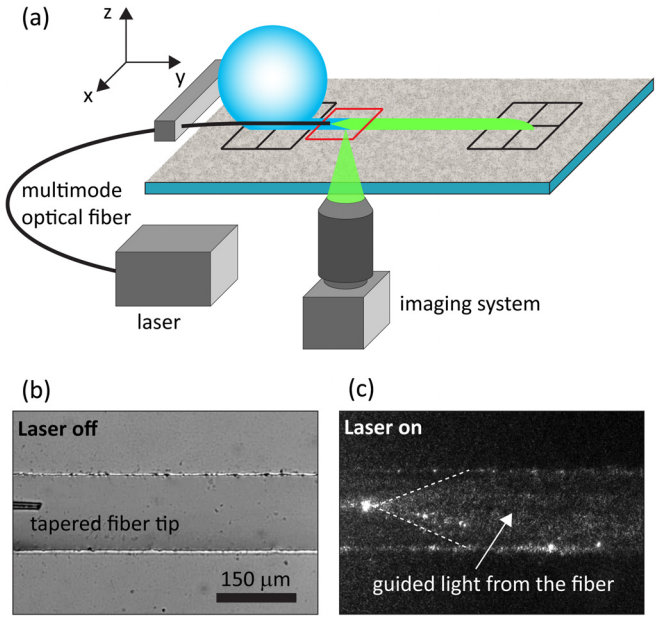

FIG. 4. (a) Light coupling into a surface-supported optofluidic waveguide via a tapered multimode optical fiber. (b) Bright field image of ethylene glycol filament with inserted tapered optical fiber and laser turned off. (c) Scattered light image of the same region as in (b) with laser turned on. Surface regions shown in (b) and (c) correspond to the red rectangle indicated in (a).

Comparison of parts (b) and (c) clearly demonstrates confinement of the liquid to the regions of the surface where the SH layer has been removed by ablation. The transverse cross-sectional profile of the resulting ethylene glycol filament is a segment of a circle (see inset in Fig. 3(c)). Maximal height h of the filament at the center of the hydrophilic stripe with the width $w = 200\,\mu$m was estimated from fiber-positioning experiments described in the next paragraph to be $h \approx 40$–$50\,\mu$m. This gives the value of the apparent lateral contact angle $\theta = \arcsin(4hw/[w^2 + 4h^2]) \approx 43.6°$–$53.1°$.[16]

After formation of surface-supported ethylene glycol filaments, we carried out experiments aiming at the characterization of their waveguiding properties. As the refractive index of ethylene glycol ($n_L = 1.447$ at 546 nm) is higher than the refractive index of the supporting MgF_2 substrate ($n_S = 1.379$ at 546 nm), light rays incident on the liquid-solid interface with angles of incidence greater than the critical angle $\Phi_C = \arcsin(n_S/n_L) \approx 72.4°$ undergo total internal reflection. Consequently, these rays stay confined in the ethylene glycol filament and can be guided along its axis. In order to couple the light into the filament, we used a multimode optical fiber (AFS50/125 Y; Thorlabs) with a nominal numerical aperture NA = 0.22 inserted into the filament through the ethylene glycol droplet (see Fig. 4(a)). Since the diameter of the fiber (125 μm) was bigger than the typical height of the ethylene glycol filaments ($h < 50\,\mu$m), the fiber was tapered to a tip with outer diameter $\sim 15\,\mu$m which allowed full immersion of the fiber in the liquid (see Fig. 4(b)); this tapering was accomplished with heat-and-pull manufacturing technique.[17] Light from a laser diode module ($\lambda = 532$ nm, maximal power 15 mW) was coupled to the opposite end of the fiber and, subsequently, the tapered tip was positioned within the liquid filament using a 3-axis manual stage to achieve optimal coupling from the multimode fiber into the optofluidic waveguide. Upon successful coupling, scattering of guided laser light from the waveguide could be observed with a sensitive CCD camera (see Fig. 4(c)). This scattered light was only emitted from the ethylene glycol-covered regions of the patterned SH surface, consistent with the notion of the light confinement and guiding in the liquid. Manipulation of the tapered fiber tip was also used to estimate the maximal height h of ethylene glycol filaments. First, the fiber tip attached to the 3-axis manual positioning stage was aligned to be parallel to the filament axis and lifted above the filament surface. Subsequently, the fiber was gradually lowered down to the point where the tip was observed to snap into contact with the filament surface due to the formation of a liquid capillary bridge. Filament height was then determined by focusing the CCD camera consecutively at the fiber tip resting on the filament surface and at the SH substrate in the immediate vicinity of the filament and calculating the difference between the two focus positions.

In order to evaluate quantitatively the light guiding performance and losses of our optofluidic waveguides, we analyzed the light intensity distribution in scattered-light images of extended waveguides with light coupled into them. To this end, we recorded sequences of scattered-light images of partially overlapping waveguide regions and then combined these partial images together using MosaicJ plugin for ImageJ image analysis software.[18] To avoid intensity background arising from the forward-scattered light emanating directly from the tapered fiber tip, we performed the analysis of propagation losses for curved optofluidic waveguides of sigmoidal shape illustrated in Fig. 5(a). In Fig. 5(b), scattered-light image of the waveguide shown in Fig. 5(a) is presented. This image clearly visualizes guided laser light that propagates along the full length of the curved waveguide. Figure 5(c) summarizes the variation of intensity I of the scattered light along the waveguide axis indicated by dashed-dotted red curve in Fig. 5(a). At each point on the waveguide axis, the average intensity I was calculated as the

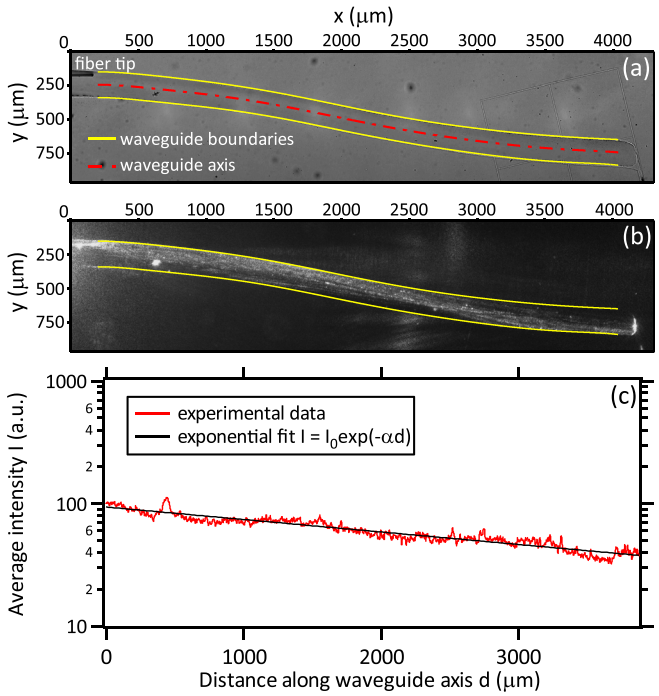

FIG. 5. (a) Bright field image of curved ethylene glycol waveguide with inserted tapered optical fiber and laser turned off. (b) Scattered light image of the same waveguide as in (a) with laser turned on. (c) Variation of intensity I of the scattered light along the waveguide axis denoted by red dashed-dotted line in (a).

mean intensity value along a line spanning the whole width of the waveguide and perpendicular to the waveguide axis at the given point on the axis. The experimental data (red curve) were fitted with an exponential curve of the form $I(d) = I_0 \exp(-\alpha d)$ (black line), where d denotes the distance along the waveguide axis. For the particular data set shown in Fig. 5(c), the fit gave $\alpha = 2.348\,\mathrm{cm}^{-1}$ which can be translated into the waveguide propagation loss of $\eta = -10\alpha/\ln 10 = -10.2\,\mathrm{dB\,cm}^{-1}$. Similar propagation loss values were obtained for various optofluidic waveguides of the same geometry (width, radius of curvature). This value of the propagation loss compares favorably to the propagation loss of $-13\,\mathrm{dB\,cm}^{-1}$ observed by Jain *et al.* with hydrogel-based multimode optical waveguides.[12]

In summary, we introduced free-standing optofluidic waveguides based on ethylene glycol filaments that were generated by controlled wetting of MgF_2 substrates with surface wettability patterned by femtosecond-laser ablation. We demonstrated straightforward formation of well-defined, millimeter-sized curved liquid filaments, and efficient light coupling into the filaments. Light guiding experiments then proved that such filaments can be successfully used to direct light along the substrate surface with relatively low propagation losses. Even though we employed transparent MgF_2 plates as the basic low-refractive-index substrate, our fabrication and characterization techniques are applicable to a wide range of solid substrate materials including opaque ones (e.g., teflon). Patterning of the surface wetting properties by laser ablation is fast and allows creation of arbitrary 2-D patterns including branched waveguides. Liquid filaments formed on such patterned surfaces can then serve as flexible on-chip optofluidic components that allow, for example, direct embedding of living biological cells into them.

This work was partially supported by the Scientific and Technological Research Council of Turkey (TÜBITAK, Grant No. 112T972) and Turkish Academy of Sciences (TÜBA GEBIP). We thank Yasin Karadag for preparing tapered multimode optical fibers and Ugur Unal for recording SEM images of superhydrophobic surfaces.

[1]D. Psaltis, S. R. Quake, and C. Yang, Nature **442**, 381 (2006).
[2]C. Monat, P. Domachuk, and B. J. Eggleton, Nat. Photonics **1**, 106 (2007).
[3]X. Fan and I. M. White, Nat. Photonics **5**, 591 (2011).
[4]D. Brennan, J. Justice, B. Corbett, T. McCarthy, and P. Galvin, Anal. Bioanal. Chem. **395**, 621 (2009).
[5]D. Zhang, L. Men, and Q. Chen, Sensors **11**, 5360 (2011).
[6]*Microfluidic Technologies for Miniaturized Analysis Systems*, edited by S. Hardt and F. Schönfeld (Springer, 2007).
[7]B. Zhao, J. S. Moore, and D. J. Beebe, Science **291**, 1023 (2001).
[8]P. Lam, K. J. Wynne, and G. E. Wnek, Langmuir **18**, 948 (2002).
[9]H. Gau, S. Herminghaus, P. Lenz, and R. Lipowsky, Science **283**, 46 (1999).
[10]A. A. Darhuber, S. M. Troian, S. M. Miller, and S. Wagner, J. Appl. Phys. **87**, 7768 (2000).
[11]S. Xing, R. S. Harake, and T. Pan, Lab Chip **11**, 3642 (2011).
[12]A. Jain, A. H. J. Yang, and D. Erickson, Opt. Lett. **37**, 1472 (2012).
[13]A. Kiraz, A. Kurt, M. A. Dündar, and A. L. Demirel, Appl. Phys. Lett. **89**, 081118 (2006).
[14]K. Mann, G. Pfeifer, and G. Reisse, "Laser-induced damage in optical materials," Proc. SPIE **1848**, 415–423 (1993).
[15]R. R. Gattass and E. Mazur, Nat. Photonics **2**, 219 (2008).
[16]A. A. Darhuber, S. M. Troian, and W. W. Reisner, Phys. Rev. E **64**, 031603 (2001).
[17]J. C. Knight, G. Cheung, F. Jacques, and T. A. Birks, Opt. Lett. **22**, 1129 (1997).
[18]P. Thevenaz and M. Unser, Microsc. Res. Tech. **70**, 135 (2007).